Effects on Dimensional Accuracy of Microstereolithographically Machined Parts after Addition of Light Absorber

M. M. Zabti
Advanced Centre of Technology
Tripoli - Libya
m.zabti@gmail.com

M. EM. Abid
University of Tripoli
Tripoli - Libya
mahmal0365@yahoo.com

M. A. Nwir
College of Engineering Technology
Janzour - Libya
mohnowar@yahoo.com

Abstract —**The paper's aim is to investigate the influence of added light absorber (Tinuvin® 327) on dimension accuracy of three-dimensional (3D) micro-parts manufactured by a dynamic mask projection microstereolithography (μSL) system. One of the common problems with stereolithography systems, and particularly with μSL is the uncontrolled cure depth of the UV light when fabricating down-facing surfaces. To overcome this problem, light absorber is commonly used to control the cure depth. Yet the influence of light absorber on the dimension accuracy of manufactured parts is not fully understood and needs to be investigated. This work explores the effect on part accuracy of adding four different concentrations of Tinuvin®327 to PIC-100 acrylate resin without light absorber. A benchmark part has been designed to evaluate the effect of the added Tinuvin®327 on linear, position, and geometric dimensions. Results show that Tinuvin®327 has significant effects on part accuracy.**

Index Terms: **photo-polymerisation,Tinuvin®327, PIC-100, microstereolithography.**

I. INTORDUCTION

3D systems Inc. introduced stereolithography (SL) into the first commercial SFF (Solid Freeform Fabrication) machine system in 1988. [1, 2]. This SL system is still being used today, and is capable of producing accurate parts. SL uses an optical system to focus an ultraviolet laser beam on a liquid resin surface and then scans a sliced 3D model to solidify the liquid resin and create solid parts with accurate dimensions. SL systems are capable of producing very accurate parts compared with other RP systems, but not at the micro-scale due to the recoating system used in SL machines, which could damage micro-features.

In 1993, Ikuta et al. suggested an alternative micro stereolithography machine (μSL) system. Initially these were based on a line-scan method where a UV laser scanned the resin surface line by line. Later, in 1996 Nakamoto and Yamaguchi, developed the first mask-based μSL system [2]. In this system, instead of scanning line by line the complete sliced layer was projected onto the resin surface. There was a significant enhancement in resolution when Maruo et al. (1997) suggested the two-photon absorption method, where photo polymerisation is activated by focusing a near infrared pulsed laser beam through an objective lens. 3D component parts are constructed by scanning the focused spot in three dimensions inside the resin [3]. The liquid crystal display (LCD) was introduced by Bertsch et al. (1997). Here, dynamic mask generators are used to project the required pattern onto the resin surface. First, they used a LCD and then in 2001 a digital micro-mirror device (DMD) was proposed [4]. Both the LCD and DMD are referred to as projection methods and are different from the vector scanning method. Many researchers have developed similar but more advanced and newer μSL techniques, and produced better-quality μSL systems for fabricating complex micro features [5,6] One of these latest techniques is the Perfactory® machine from Envision TEC. The Perfactory® is a μSL mask projection machine. It uses a 250W UHP (ultra high pressure) lamp as a UV source to solidify the resin by projecting the UV light through a window underneath the resin vat. The Perfactory® is provided with an electro-mechanical shutter, which is used to expose the resin for the required duration necessary for it to solidify.

A. Definition of the Problem

In order to fabricate a microstructure part with μSL, the designed 3D model has to be sliced to desired layer thickness, and each cured layer must be bonded with the previous sliced layer during solidification to complete the design geometry. To fabricate these thin slices in the correct manner, the cure depth (Cd), defined, as the depth to which a 3-D polymerisation network is formed during the process [7], has to be similar to the slice thickness. The two parameters that describe curing characteristics of a resin are penetration depth (Dp, the depth at which the beam intensity is reduced to 1/e its intensity at the surface), and critical energy (Ec, energy required for the transition of the resin from liquid phase to solid phase, the irradiation energy at which the cure depth of the material is zero). Dp and Ec are used to determine the exposure energy (Ex) for fabricating the thin layers and bonding them together. Various earlier researchers have reported the use of different forms of light absorbers or

Received 18 March 2015; revised 11 April 2015; accepted 23 April 2015.
Available online 01 July 2015.

polymerization inhibitors in attempts to control cure depths in µSL systems, and which have led to reproduction of more accurate feature details.

A.1. Causes of Overcure

In µSL systems the thickness of the layer to be polymerized is given by the depth of resin between the last cured layer and the vat surface [8]. Any excess of radiation increases the curing of the previous layer. However, if the part is designed to contain overhangs or bridges the radiation penetrating upwards into the resin vat causes an increase in the thickness of the hanging layer which affects the vertical resolution. The vertical resolution has considerable impact on the ability of µSL to reproduce 3D microstructures accurately [8]. Many undesired microstructures could be 'fabricated' if the cure depth is greater than the slicing thickness. Geometric and dimensional accuracy will be influenced by this over-penetration. In order to successfully fabricate 3D microstructures with down-facing surfaces, the cure depth must be controlled by adjusting the curing characteristics.

Zissi et al. (1996) derived the cure depth and width as functions of light absorption concentration [9]. Choi et al, (2009), used Tinuvin® 327 as a light absorber to control cure depth in an attempt to accurately fabricate 3D parts with down-facing surfaces [8]. Different concentrations of Tinuvin®327, were mixed into an acrylate-based photo curable resin and tested for the successful fabrication of micro-parts with overhanging features. Results showed that, Tinuvin® 327 effectively controlled UV penetration in µSL.

A.2. Critical Energy

As shown in Eq. (1), the cure depth is proportional to the logarithm of Emax/Ec (where Emax is the maximum exposure energy at the centre of irradiated zone):

$$Cd = Dp \ln\left(E_{max}/Ec\right) \qquad (1)$$

When a semi-logarithmic graph of C*d* verses ln (E*c*) is plotted, Figure 1, the result is a straight line with gradient equal to the value of D*p*. E*c*, the critical energy at which the cure depth is zero, is given by the intersection of the line with the abscissa. Because the curve is dependent only on the resin constants E*c* and D*p*, it is characteristic for resin and is also called a 'working curve' [1].

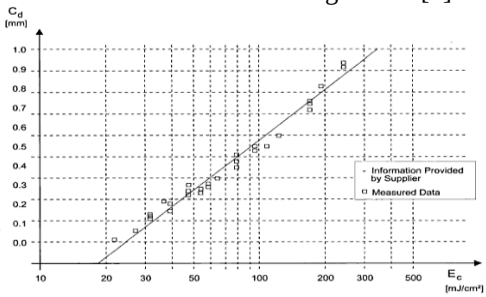

Figure 1. Cure Depth As A Function Of Exposure Energy, Working Curve For HS 660 Resin [1].

More recent research (5) and (8) has raised the essential question: does adding a light absorber have any effects on dimension accuracy? This research is aiming at devoting an answer to this question. More particularly, it is focused on the effects of different concentrations of light absorber on linear form, and position dimensions of the produced parts.

II. EXPERIMENTAL WORK

The experimental work reported in this paper was conducted using an Envision TEC® Mini Multi Lens machine, and investigated the effect on the accuracy of the parts produced, of adding different concentrations of Tinuvin® 327 as a light absorber to PIC-100 acrylate resin. The pure PIC-100 resin was supplied by Envision TEC® and the light absorber, Tinuvin®327, supplied from Atlas Chemicals Ltd, as a fine yellow powder.

A. Materials Preparation

In addition to the resin without light absorber, four different concentrations of Tinuvin® 327 (0.1, 0.25, 0.5 and 1.0% w/w) were added to the resin Tinuvin® 327 were dissolved in chloroform (CHCl3) and then mixed with PIC-100 acrylate resin in a roller for 12 hours to obtain a homogenous distribution of the ingredients and allow the chloroform to evaporate.

B. Benchmark Design

Based on an extensive literature study, and discussions with other workers in the field, a 3-D benchmark design was developed which allowed evaluation of certain common dimensional and geometric features to ascertain µSL part accuracy before and after the addition of Tinuvin®327.

Linear dimensions are classified according to small, medium and large distances (S, M, and L). The design benchmark proposed, see Figure 2, consists of a square base of 10 000 µm length, 10 000 µm width, and 2 000 µm thickness. To assess accuracy of linear dimensions and ensure repeatability, a cuboid boss of side length 2000 µm, was added to each corner of the design. Two of these cubes were designed with positive portions (cubes and cylinders) to stand proud of the base. Other two cubes were designed as insertions into the base (cubes and cylinders), to assess the effect of addition of light absorber on the formation of positive and negative geometric features, and to assess the effect of Tinuvin®327 on position dimensions in terms of coaxiality.

Table 1. Position Dimension Group

No	Class	Distance	Nominal Value (µm)
17	coaxiality	Centre of Large hole with small hole	0
18	coaxiality	Centre of Large cylinder with small cylinder	0

Table 2. Form Dimension Group

No	Class	Distance	Nominal Value (µm)
13	Circularity	Large cylinder portion	0
14	Circularity	Small cylinder portion	0
15	Circularity	Large cylinder hole	0
16	Circularity	Small cylinder hole	0

Table 3. Linear Dimension Group

No	Class	Distance	Nominal Value (µm)
1	L	Outside X	10 000
2	L	Outside Y	10 000
3	M	Between cubes	6 000
4	M	Between cubes	6 000
5	S	Large square boss length	2 000
6	S	Large square boss width	2 000
7	S	Small square boss length	1 000
8	S	Small square boss width	1 000
9	S	Large square hole length	1 000
10	S	Large square hole width	1 000
11	S	Small square hole length	500
12	S	Small square hole width	400

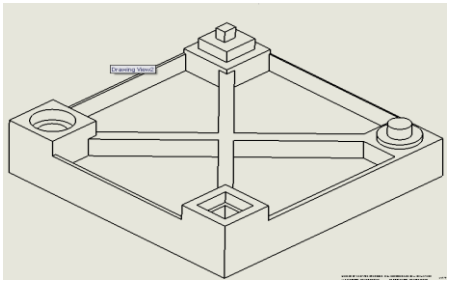

Fig.ure 2. Isometric View For The Benchmark

The top surface of the two portions (cube and cylinder) and the upper surface of the test part were used to measure surface roughness. In addition, the four cubes were used to assess distance measures. To structure the measurement process these features were classified as: the linear dimension group (XY dimensions), the Geometric (form) group, and the Position group, see the tables (1-2-3). The dimensions assigned to individual features are all in µm.

C. Fabrication of Test Part

All test parts were fabricated using the Mini Multi Lens Prefatory® machine from Envision TEC®, described above [10]. Acrylate PIC-100 resin was polymerized with fixed UV irradiance of 750 MW/dc² and 50 µm layer thicknesses. The irradiation parameters were selected and set as recommended by the resin supplier Envision TEC®.

D. Number of Specimens

For an adequate sample size of test parts, fifteen samples of an evaluation box of 20 000 µm x 15 000 µm x 10 000 µm were fabricated and evaluated using a Quick Vision® CMM machine for measuring the differences between the CAD model and the actual part dimensions. Statistical analyses were carried out using MiniTab® version 16. The error was computed using the following equations:

$$\text{Error} = \text{Actual measurement} - \text{Specified length of 3D model} \quad (2)$$

The average error for dimensional accuracy is shown in Figure 3. The figure shows that there is a number of samples where the average error becomes independent of sample size. It can be seen that after six samples the gradient of the average error curve becomes insignificant or zero. Hence, the sample size in all tests carried in this research was eight.

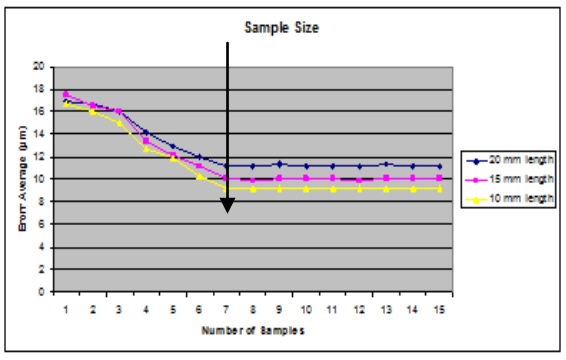

Figure 3. The Error Average For Dimensional Accuracy.

E. Measurements

To reduce human error associated with the measuring procedure and to better assure measurement precision, all linear form and position measurements were made using the Quick Vision® Machine. The quoted accuracy of the

Quick Vision® machine system is ± 2µm for the size of measurement used in this research [11].

E.1. Measurement uncertainty

To minimise the measurement error, all the measurements were taken under the maximum magnification allowed by the Quick Vison® (CMM) software. However, it is still necessary to calculate the measurement uncertainty associated with a measurement procedure used to inspect the micro features. This assessment was carried out using an existing method for calculating uncertainty [12]. It was assumed that the sources of uncertainty in inspecting the micro features were the same for all the measurements. Hence, the formula for calculating the standard uncertainty, u, is [12]:

$$u = \frac{s}{\sqrt{n}} \qquad (3)$$

Where *s* is the estimated standard deviation and *n* is the number of measurements in the set.

To carry out this assessment, and in an attempt to minimise the huge amount of data acquired, two extremes, the lowest and the highest value, with one in between were measured. Six readings were conducted for each dimension in order to judge measurement uncertainty. Table 4 shows the results of these measurements. For the dimensions with mean values of 9976 µm, 1987 µm and 975 µm, the estimated standard deviations, *s*, was calculated to be 9.1 µm, 6.1 µm and 4.1 µm, respectively, while the standard measurement uncertainties were 3.7 µm, 2.1 µm and 1.6 µm, respectively. As expected, there is an inverse relationship between the measurement uncertainty and the nominal dimensions. It was determined that the maximum measurement uncertainty was 3.7 µm for the 1 000 µm dimension which was considered acceptable for this study [12].

Table 4: Results Of Measurement Uncertainty.

Nominal Dimension µm	Measured Dimension µm	Std. dev, *s*	Std. uncertainty, u
10 000	9976	9.1	3.7
2 000	1987	6.1	2.1
1 000	975	4.1	1.6

E.2 Measurement of Circularity Errors

Circularity errors are geometric tolerances that describe by how much a circular feature deviates from a perfect circle. According to ISO 1101 circularity error is the difference in radii between two concentric circles separated by the minimum possible distance containing all the measurement points on the given profile [13], see Figure 4. [14]. Circularity errors were measured by the QuikVison® CMM machine by touching the outside of the cylinder Fig. 5 in at least three points while fixing the Z movement of the prop, then the software calculated the error in circularity.

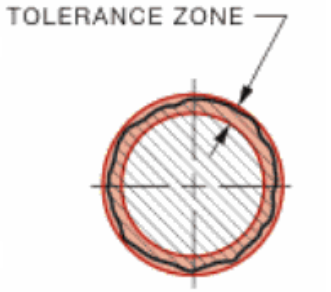

Figure 4. Circularity Error Measurement [14]

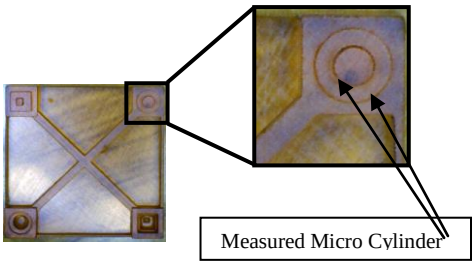

Figure. 5. Measured micro cylinders

III. RESULTS AND DISCUSSION

A.1. Linear Dimensions Error

Figure 6 shows that the addition of Tinuvin®327 has a significant effect on linear dimensional accuracy, for all the tests. The greater the concentration of added Tinuvin®327, and the greater the length of the sample, the greater the error. For the 400 and 500 µm, linear dimensions Fig. (6-a) and b, the mean error ranged from 20 µm or less for zero Tinuvin to 78 µm with 1% Tinuvin concentration. For the 1 000 and 2 000 µm linear dimensions, (Fig 6-c and d) the mean error ranged from 25 µm for zero Tinuvin, to 96 µm with 1% Tinuvin concentration. For the 6 000 and 10 000 µm linear dimensions (Fig 6-e and f), the mean error ranged from 30 µm for zero Tinuvin to 180 µm with 1% Tinuvin concentration.

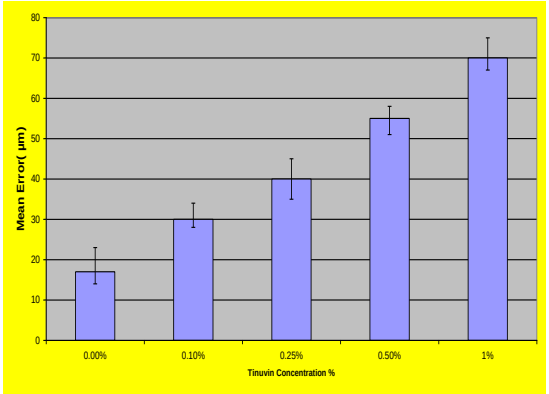

Figure. 6-a . Mean Error For 400 µm Linear Dimensions.

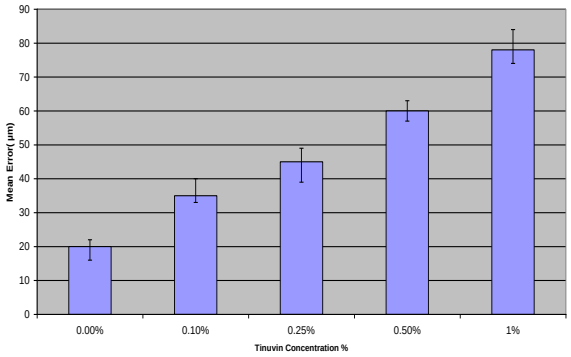

Figure 6-b . Mean Error For 500 µm Linear Dimensions.

.

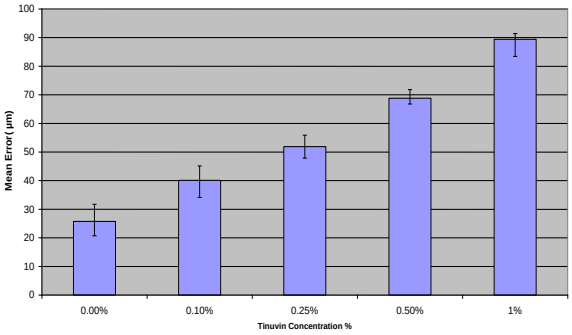

Figure 6-c . Mean Error For 1 000 µm Linear Dimensions

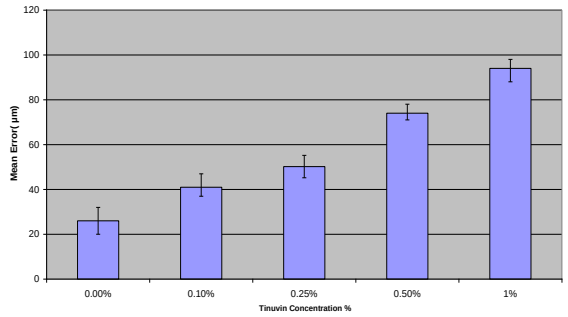

Figure 6-d . Mean Error For 2 000 µm Linear Dimension.

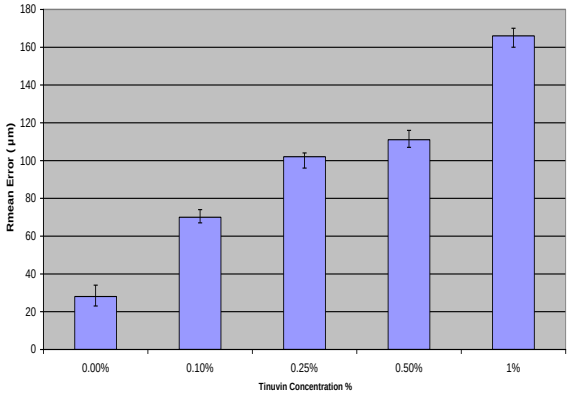

Figure 6-e . Mean Error For 6 000 µm Linear Dimension.

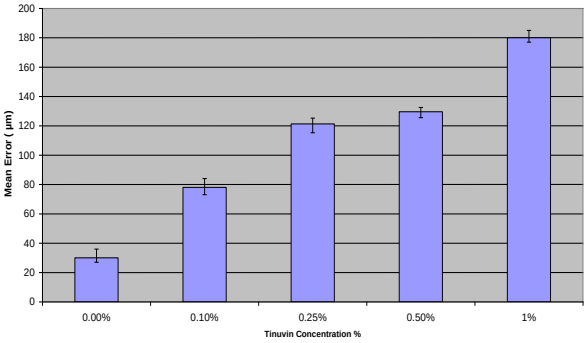

Figure 6-f . Mean Error For 10 000 µm Linear Dimension

Figure 7 presents the combined data in terms of percentage Tinuvin®327 concentrations. It is immediately obvious that the increase in the added Tinuvin®327 increased the mean error. This is due to the increased shrinkage associated with adding Tinuvin® 327 to the acrylate resin and the resulting reduction in the degree of poly-merisation and cross-linking density of the thermoset resin when light absorber is introduced into the compound [15].

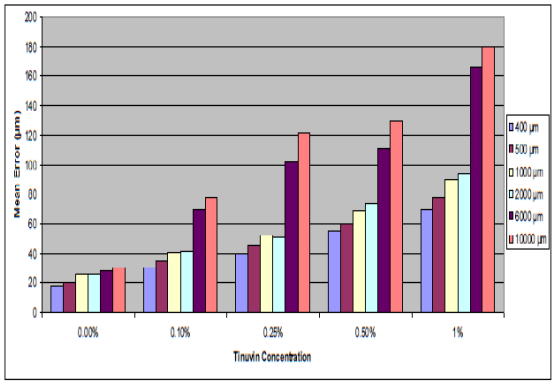

Figure 7 . Comparison Of The Effect Of Tinuvin®327 Concentration On The Linear Dimension.

A.2. Circularity and Position Error

The results for RMS errors for circularity and position measurement are shown in Figure 8 and 9. The RMS circularity error for Tinuvin concentrations of 0.0, 0.1, and 0.25%, ranges between 19 and 22 µm, which increases to 55 µm at 1% concentration. For position error the minimum RMS error was 6 µm for 0% Tinuvin concentration and a maximum RMS error of 16 µm for 1.0% Tinuvin. For concentrations less than 0.25% decrease in the Tinuvin®327 concentration causes no significant change in roundness or position error.

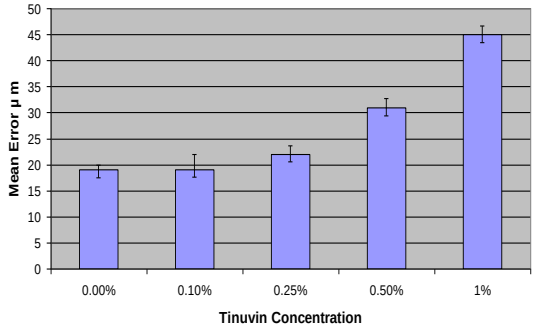

Figure 8 . Circularity Measurement Errors

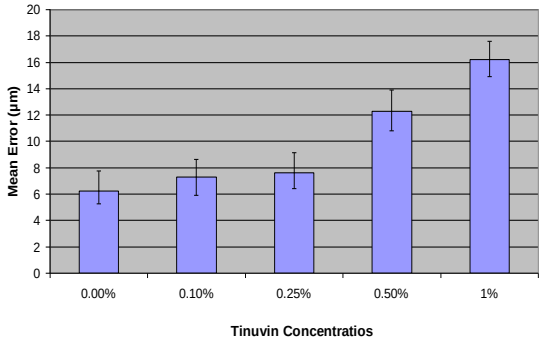

Figure 9 . Position Measurement Errors

IV. CONCLUSION

This paper has investigated the effect of Tinuvin®327 concentration on part accuracy in µSL. PIC-100 acrylate resin with different Tinuvin concentrations was used to study the relationship between light absorber concentration and part accuracy in terms of linear dimensions, form, and position. Results show that Tinuvin®327 has a significant effect on dimension accuracy. For linear dimensions the error increased with length of the part and the amount of Tinuvin added, due to the shrinkage associated with adding Tinuvin® 327 to acrylate resin. Tinuvin®327 has no significant effect on either roundness and position error when the concentration was less than 0.25%, but the error becomes obvious at 0.5% Tinuvin concentration.

REFERENCES

[1] Chua, C., Leong, K., Lim, C. (2003) Rapid Prototyping: Principles and Applications, World Scientific Publishing, Singapore.

[2] Gebhardt, A. (2000) *Industrial* rapid *prototyping systems*, Rapid Prototyping, 2nd Ed., Hanser, Berlin, pp. 81-235.

[3] Maruo SO, Nakamura, O, Kawata K. 1997. Three-dimensional microfabrication with two-photon absorbed photo polymerization. Opt. Lett 22:132–134.

[4] Bertsch, A., Zissi, S., Jezequel, J.Y., Corbel, S. Andre, J.C., "*Microstereolithography:* Concepts *and applications,"* Proc. 8th IEEE Int. Conference on Emerging Technologies and Factory Automation, 2001, pp. 289~298.

[5] Bertsch, A., Jiguet, S., Bernhard, P., Renaud, P. (2003) "*Micro stereolithography: a review"*. Symposium on Rapid Prototyping Technologies, *Materials Research Society Symposium Proceedings*, December 3-5, 2002. Boston.

[6] Sun, C., Fang, N., Wu, D., Zhang, X. (2005) *"Projection micro-stereolithography using digital micromirror dynamic mask"*, Sensors and Actuators A: Physical, Vol. 121 No. 1, pp. 113-20.

[7] Lee, J.H., Prud'homme, R.K., Aksay, I.A. (2001) "Cure depth in photo polymerization: Experimental and theory", J Mater. Res. 16 (2001), pp. 3536–3544.

[8] Choi, J-W., Wicker, R., Cho, S-H., Ha, C-S., Lee, S-H. (2009) "Cure depth control for complex 3D microstructure fabrication in dynamic mask projection micro stereolithography", Rapid Prototyping Journal, Vol. 15 No.1, pp. 59-70.

[9] Zissi, et al (1996) "Stereolithography and micro techniques", Microsystem Technologies, Vol. 2 No.2, pp. 97-102.

[10] Envision TEC®. (2008) "Computer-aided Modelling Devices" [Online] Available from www.envisiontec.com/index.php. [Accessed: 12/Jun/2010].

[11 Mitutoyo 2010 http://www.mitutoyo.co.uk/Mit/downloads/vision/QVElf.pdf [Accessed:1/Dec/2010].

[12] Kirkup, L., and Frenkel, B., (2006) "An Introduction to Uncertainty in Measurement," Cambridge University Press.

[13] International Standard ISO 1101 (1983) "Technical Drawings - Geometrical Tolerancing", ISO 1101 (1983) 12-01.2.

[14] Jensen, C., Helsel, J., Espin, E. (2011) "Interpreting Engineering Drawings" 6th Canadian edition.

[15] Pilkenton, M., Lewman, J., Chartoff, R. (2011) "Effect of oxygen on the crosslinking and mechanical properties of a thermoset formed by free-radical photocuring " Journal of Applied Polymer Science, Volume 119, Issue 4, pp. 2359–2370.